

Deciphering high-pressure metamorphism in collisional context using microprobe mapping methods: Application to the Stak eclogitic massif (northwest Himalaya)

Pierre Lanari¹, Nicolas Riel¹, Stéphane Guillot¹, Olivier Vidal¹, Stéphane Schwartz¹, Arnaud Pêcher¹, and Keiko H. Hattori²

¹ISTerre, University of Grenoble 1, CNRS, 1381 rue de la Piscine, 38041 Grenoble, France

²Department of Earth Sciences, University of Ottawa, Ottawa, Ontario K1N 6N5, Canada

ABSTRACT

The Stak massif, northern Pakistan, is a newly recognized occurrence of eclogite formed by the subduction of the northern margin of the Indian continent in the northwest Himalaya. Although this unit was extensively retrogressed during the Himalayan collision, records of the high-pressure (HP) event as well as a continuous pressure-temperature (P - T) path were assessed from a single thin section using a new multiequilibrium method. This method uses microprobe X-ray compositional maps of garnet and omphacitic pyroxene followed by calculations of $\sim 200,000$ P - T estimates using appropriate thermobarometers. The Stak eclogite underwent prograde metamorphism, increasing from 650 °C and 2.4 GPa to the peak conditions of 750 °C and 2.5 GPa, then retrogressed to 700–650 °C and 1.6–0.9 GPa under amphibolite-facies conditions. The estimated peak metamorphic conditions and P - T path are similar to those of the Kaghan and Tso Morari high- to ultrahigh-pressure (HP-UHP) massifs. We propose that these three massifs define a large HP to UHP province in the northwest Himalaya, comparable to the Dabie-Sulu province in China and the Western Gneiss Region in Norway.

INTRODUCTION

The recent discovery of microdiamond and coesite inclusions in rocks previously considered as collision-type granulites (Kotkova et al., 2011) suggests that evidence for subduction-related metamorphism is commonly obliterated during late collisional events. Le Fort et al. (1997) considered that the Stak massif in northern Pakistan (Fig. 1) is a retrogressed eclogitic massif, but the pervasive retrogression made it difficult to evaluate the peak metamorphic conditions, which were only constrained to be >1.3 GPa and >610 °C. We report a new approach involving X-ray mapping of a single thin section, $520 \mu\text{m} \times 670 \mu\text{m}$ in size, which yielded information to determine a detailed pressure-temperature (P - T) path. This path is similar to those of eclogitic units of Kaghan and Tso Morari (~ 150 km and ~ 500 km from the Stak massif, respectively), which suggests the presence of a large high-pressure (HP) to ultrahigh-pressure (UHP) province in the northwest Himalaya.

GEOLOGICAL SETTING AND SAMPLE DESCRIPTION

The Stak area is located in the Indus valley northwest of Skardu, Pakistan (Fig. 1). High-pressure rocks are exposed on the northern edge of the Indian continental plate within the Main Mantle Thrust, between the Ladakh arc to the south and the Nanga Parbat–Haramosh gneisses (Higher Himalayan crystallines) to the north (Fig. 1B). These units (weakly metamorphosed garnet-free amphibolites of the Ladakh arc, strongly metamorphosed metasedimentary rocks of the Nanga Parbat, and felsic gneisses of the Nanga Parbat core) are imbricated in tight, multiphase folds up to a kilometer in scale with superimposed NNE-SSW and east-west trends. Mafic dikes that originally intruded the sedimentary rocks form metric to decametric eclogitic boudins within the felsic gneisses in an area ~ 2 km wide by ~ 10 km long, with poorly delineated boundaries (Guillot et al., 2008); this area is defined as the Stak massif. Our investigation focused on these eclogitized mafic boudins, which contain layers of small rounded garnet and omphacitic pyroxene. The cores are rimmed by hydration prod-

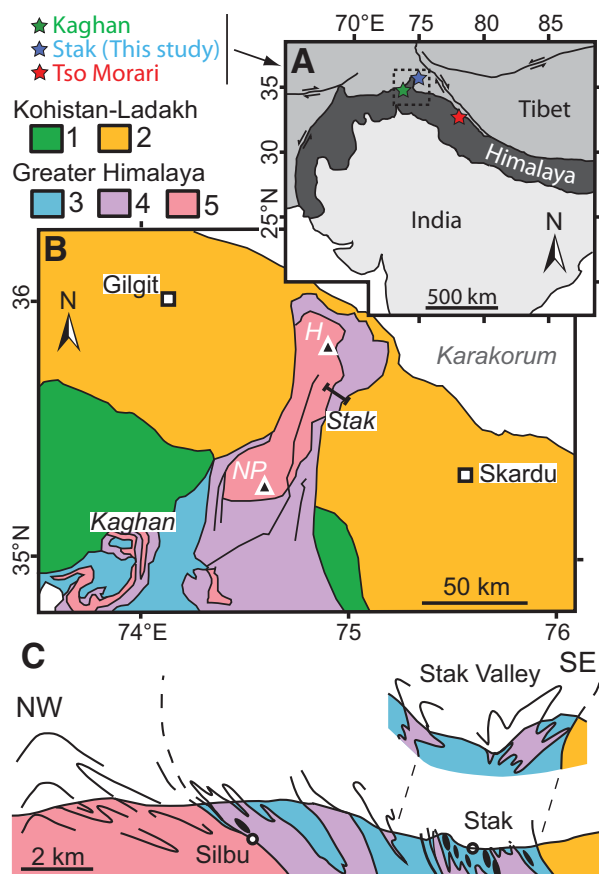


Figure 1. A: Map of northern India and Himalaya area with locations of known eclogitic massifs (Tso Morari, Kaghan, and Stak). B: Northwest Himalayan massif, modified from Pêcher et al. (2008). NP—Nanga Parbat; H—Haramosh. C: Cross section through the Stak massif. Geological units: 1—amphibolites (Kohistan) and Chilas complex (Ladakh); 2—undifferentiated Kohistan and Ladakh units (volcano and metasediments, batholiths, and Eocene volcanics); 3—Neotethyan sedimentary group; 4—Higher Himalayan crystallines and Paleozoic intrusives; 5—basement gneiss.

ucts of amphibole and biotite formed during the Himalayan collision. Sensitive high-resolution ion microprobe (SHRIMP) dating on zircon yielded scattered Himalayan ages between 70 and 50 Ma (Riel et al., 2008).

Samples show evidence for three deformation events, with each represented by a specific paragenesis. An early paragenesis (P1) consists of garnet with phengite inclusions and relict omphacitic pyroxene in small areas ($<1 \text{ mm}^2$) in the matrix. Omphacite is partially replaced by symplectic intergrowths of secondary pyroxene, plagioclase, and amphibole (Fig. 2). The foliation associated with P1 is defined by the preferred orientation of omphacite and garnet. A later paragenesis (P2) is composed of millimetric amphibole and biotite in discontinuous layers along the main

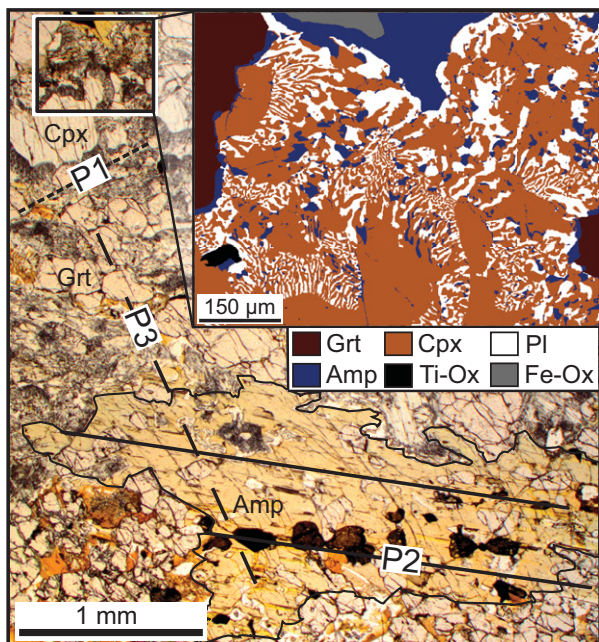


Figure 2. Photomicrograph showing the texture of the studied sample. Three main parageneses were identified (labeled P1, P2, and P3; see text). Inset shows mapped area. Grt—garnet; Cpx—clinopyroxene; PI—plagioclase; Amp—amphibole; Ti-Ox—Ti-oxide; Fe-Ox—Fe-oxide.

foliation (Fig. 2). The third paragenesis (P3) consists of calcite and chlorite, which developed at the expense of garnet along fractures.

MICROPROBE MAPPING AND TREATMENT METHODS

A JEOL JXA-8200 electron probe microanalyzer at the Institute of Earth and Environmental Science, Potsdam University (Germany), was used to acquire spot analyses and X-ray compositional maps in wavelength-dispersive mode (De Andrade et al., 2006; Lanari et al., 2012a). Analytical conditions for spot analyses were 15 keV accelerating voltage and 10 nA specimen current. Standards used were Fe_2O_3 (Fe), MnTiO_3 (Mn, Ti), diopside (Mg, Si), orthoclase (Al, K), anorthite (Ca), and albite (Na). The compositional mapping of 350,000 pixels over an area of $520 \mu\text{m} \times 670 \mu\text{m}$ was carried out at 200 ms per pixel (see De Andrade et al., 2006, for a detailed statistical evaluation). Higher specimen current of 100 nA was employed for mapping. During the mapping, spot analyses were also conducted along profiles in the analyzed area. The data were then used to calibrate the X-ray compositional maps.

The X-ray compositional maps were treated using a MATLAB®-based software, XMapTools, which identifies mineral phases and their locations from X-ray images (Lanari et al., 2012b). In the program, the raw data were converted to quantitative concentrations using the results of spot analyses (one for each phase in the sample), and a structural formula was calculated for each pixel of the mapped area. Each mineral was separated into different compositional groups (for example, clinopyroxene was divided into four subgroups based on the Na and Fe contents). Finally, P - T conditions were calculated in XMapTools using empirical and semiempirical thermobarometers.

CHEMICAL AND THERMOBAROMETRY RESULTS

Garnet shows similar compositions from core to rim ($\text{Alm}_{48} \text{Prp}_{32-33} \text{Grs}_{17-19} \text{Sps}_5$) with the exception of a thin (15 μm) rim that contains low pyrope (29%) and grossular (16%), and higher almandine and spessartine. The rim likely formed by reactions with amphibole during the late P3 event. Phengite enclosed in garnet has intermediate Si content, 3.28 per

formula unit (p.f.u.). Four groups of clinopyroxene were identified. Primary clinopyroxene has high jadeite content ($\text{Jd}_{41}\text{--Jd}_{40}$ corresponding to omphacite) and shows an increase in Fe from 0.07 p.f.u. in the core to 0.19 p.f.u. in the rim. The primary clinopyroxene is further divided into two subgroups based on the Fe contents, 0.07–0.13 and 0.13–0.19 p.f.u. The secondary clinopyroxene in symplectite is divided into two subgroups, one with high jadeite content ($\text{Jd}_{30}\text{--Jd}_{25}$) and the second with low jadeite content ($\text{Jd}_{25}\text{--Jd}_{10}$). This decrease in jadeite content correlates with the decreasing width of intergrowths. Plagioclase in symplectites has similar compositions from core (Ab_{87}) to rim (Ab_{85}). Three groups of amphibole were identified. The first group comprises small grains (10–30 μm) in the symplectite, and has low Fe^{3+} content in M1 (0.48 ± 10 p.f.u.) and a high Na content in A (0.54 ± 0.6 p.f.u.). The second group has a larger grain size (>100 μm) and shows higher Fe^{3+} content in M1 (0.70 ± 15 p.f.u.) and lower Na content in A (0.39 ± 15 p.f.u.). The third group occurs as corona on garnet (Fe^{3+} in M1 of 0.54 p.f.u. and Na in A of 0.30 p.f.u.). Detailed composition data are provided in the GSA Data Repository¹.

Pressure and temperature conditions were estimated for the different paragenetic sequences outlined above. The first assemblage, labeled A in Figure 3, is composed of garnet, omphacite, and phengite. Because omphacite shows a range in Fe content, the P - T conditions were estimated using varying omphacite compositions and fixed garnet and phengite compositions. The calculation used the composition of phengite with the highest Si content and the average composition of garnet. The calculation used the garnet-omphacite thermometer of Ravna (2000b), which is the latest calibration, and the garnet-omphacite-phengite barometer of Waters and Martin (1993) and Waters (1996). The calculated P - T conditions are plotted in a P - T diagram, and the pixels (~200,000) are shown in the mapped area (Fig. 3A). Omphacite crystallization started at 650 °C and 2.4 GPa (“a1”, orange-colored field in Fig. 3) and continued to form during the peak metamorphic conditions of 750 °C and 2.5 GPa (“a2”, red-colored field in Fig. 3).

The symplectite of clinopyroxene, amphibole, and plagioclase is a breakdown product of omphacite (Waters, 2003). This retrogressed assemblage is divided into two, based on crystal sizes in the symplectite; they are labeled B and C in Figure 3. Clinopyroxene grains in the symplectite assemblage B are larger and occur together with amphibole and plagioclase on the rims of relict omphacite. The second symplectite assemblage, C, has a smaller grain size. The P - T conditions reflecting this textural change were calculated using equilibria involving pyroxene, plagioclase, and amphibole in the absence of quartz. The temperature was first estimated from the distribution of Na and Ca between plagioclase and hornblende using the edenite-richterite calibration of Holland and Blundy (1994). The estimated temperatures vary from 680 °C where plagioclase is in contact with Jd_{30} clinopyroxene to 640 °C in contact with Jd_{10} clinopyroxene. Pressure was estimated with fixed composition of amphibole and plagioclase for the defined temperature ranges using the calibration of Waters (2002, 2003) based on the reaction jadeite + tremolite = albite + edenite, involving clinopyroxene, plagioclase, and amphibole. Activities of end members were calculated for amphibole and clinopyroxene following the models of Dale et al. (2000) and Holland (1990), respectively. Activity of plagioclase was assumed to be ideal. The P - T estimates and the corresponding pixels are also plotted in Figure 3 and mapped in Figures 3B and 3C. Our results show that clinopyroxene with plagioclase and amphibole in the symplectite crystallized under P - T conditions varying from 1.5 GPa and 680 °C (assemblage B) to 1 GPa and 650 °C (assemblage C).

The late assemblage (D in Fig. 3) includes large grains of amphibole (P2 in Fig. 2) and biotite, minor Fe-oxides, and quartz. The P - T conditions

¹GSA Data Repository item 2013027, details of mineral groups and pseudo-section, is available online at www.geosociety.org/pubs/ft2013.htm, or on request from editing@geosociety.org or Documents Secretary, GSA, P.O. Box 9140, Boulder, CO 80301, USA.

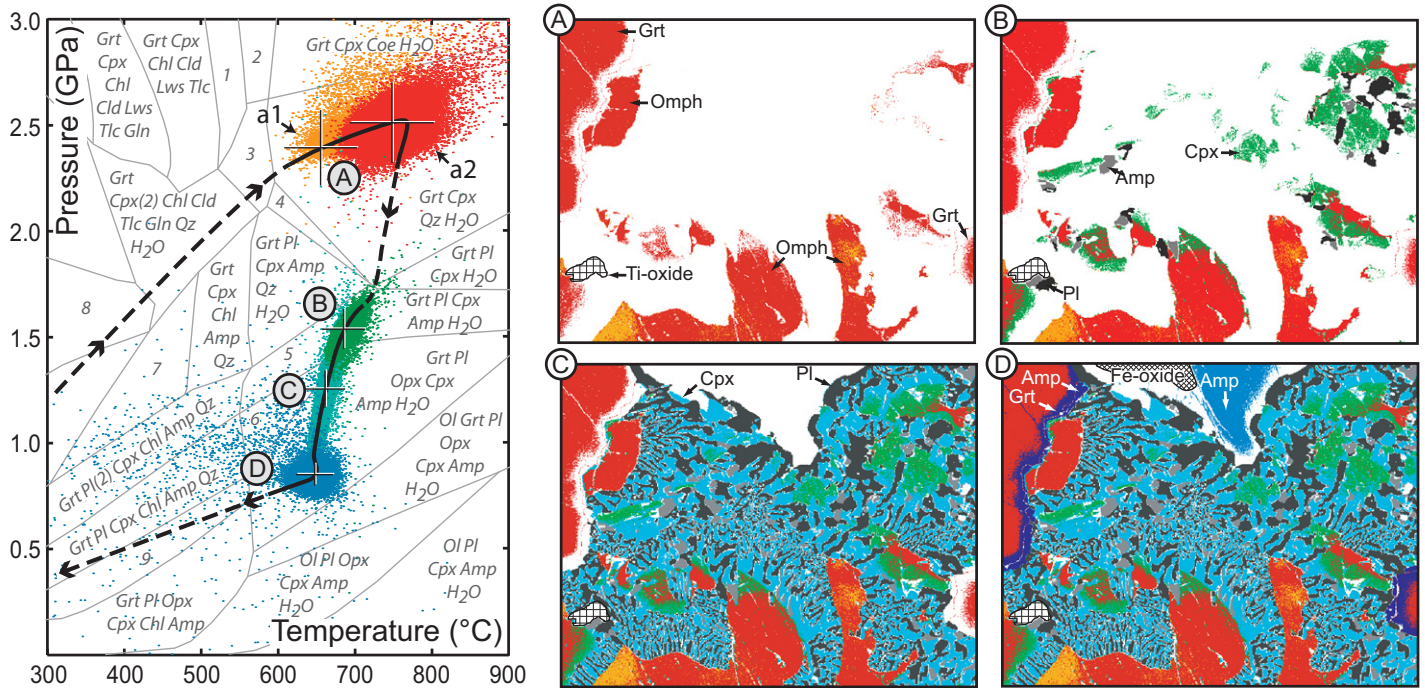


Figure 3. Pressure-temperature (P - T) grid showing estimated path of the Stak eclogite and associated P - T maps (for assemblages A, B, C, and D). Colors in maps correspond to those of fields in the P - T diagram. P - T path (thick black solid and dashed line) is based on 200,000 P - T estimates (colored dots) using empirical and semiempirical thermobarometers on a simplified pseudosection grid (see the Data Repository [see footnote 1] for the detailed grid). Error bars were estimated from the uncertainty in electron microprobe data using a Monte Carlo simulation (see the Data Repository). The clinopyroxene compositions of assemblage A are divided into two groups: a1 and a2. Grt—garnet; Cpx—clinopyroxene; Qz—quartz; Coe—coesite; Pl—plagioclase; Amp—amphibole; Ol—olivine; Chl—chlorite; Opx—orthopyroxene; Cld—chloritoid; Tlc—talc; Lws—lawsonite; Gln—glaucofanite. Complementary assemblages: 1—Grt Cpx Chl Lws Tlc H_2O ; 2—Grt Cpx Lws Coe H_2O ; 3—Grt Cpx Cld Tlc Qz H_2O ; 4—Grt Cpx Pl Qz H_2O ; 5—Grt Pl Cpx Amp Qz H_2O ; 6—Grt Pl Opx Cpx Amp Qz H_2O ; 7—Grt Cpx Chl Amp Qz Pl Gln; 8—Grt Pl Cpx (2) Cld Amp Gln Qz; 9—Grt Pl Opx Cpx Chl Amp Qz.

for the assemblage were estimated using the edenite-richterite calibration of Holland and Blundy (1994) and the barometer of Schmidt (1992). Although the Schmidt barometry is designed for granitic rocks, the observed mineral assemblage is similar to that of granulites. The results (blue pixels in Fig. 3D) show the crystallization of large amphibole grains at 650 °C and 0.85 GPa. Such conditions are common during collisional events. The Fe-Mg exchange thermometer of Ravna (2000a) yielded temperatures ranging from 510 to 460 °C for the crystallization of amphibole on the rims of garnet, which corresponds to the latest stage of exhumation.

To complement the P - T estimates, pseudosections were calculated in the NCFMASHO (Na_2O - CaO - FeO - MgO - Al_2O_3 - SiO_2 - H_2O - O) system using various software packages including Perple_X (<http://www.perplex.ethz.ch/>). Because different programs yielded similar results, the pseudosections were made with Theriak-Domino software (de Capitani and Petrakakis, 2010) using the thermodynamic database of Berman (1988). The first attempt was made using the bulk-rock composition data, but the results did not match the observed mineral abundances and mineral compositions of garnet under the HP conditions. The result indicates that the metamorphic reactions were not controlled by the bulk-rock composition. Therefore, the composition in a small area was calculated with XMap-Tools from the observed mineral compositions and abundance (50% garnet and 50% omphacite) based on the X-ray maps. The pseudosection calculated from this local bulk composition agrees well with the observed mineral compositions at pressures ranging from 2.5 to 1 GPa along the P - T path prior to hydration of the rocks at pressures of ~0.9 GPa.

METAMORPHIC AND TECTONIC IMPLICATIONS

The calculated P - T evolution shows that omphacite and garnet started to crystallize near the end of the prograde path, from ~650 °C and 2.4 GPa to up to the peak conditions at 750 °C and 2.5 GPa (Fig. 3). During this

period, garnet did not significantly change its composition, as predicted by similar compositions of garnet ($Alm_{50} Prp_{33} Grs_{16}$ at 650 °C and 2.4 GPa, and at 750 °C and 2.5 GPa) in the pseudosection (the detailed grid is available in the Data Repository). The absence of coesite in the Stak eclogite is consistent with the estimated peak pressure, which is below the stability field of coesite (Fig. 3). Symplectite intergrowth is associated with hydration, which resulted in the crystallization of amphibole. The pseudosection (Fig. 3) shows the upper stability limit of amphibole at ~1.6 GPa and 700 °C, which is in good agreement with the highest pressure for amphibole obtained by empirical barometers. The observed clinopyroxene compositions are also consistent with the calculated pseudosections. Clinopyroxene has a decreasing Na content, from 0.32 p.f.u. at 1.5 GPa and 680 °C to 0.22 p.f.u. at 1.3 GPa and 660 °C.

In summary, despite a pervasive overprint, a continuous P - T path was obtained for minerals in a single thin section from the Stak massif based on microprobe mapping data. The new approach uses the bulk compositions of small areas, the P - T conditions responsible for reactions in the small area, and microtextures, such as symplectite, to determine the reaction path; the estimated P - T path (Fig. 3) indicates that the growth of clinopyroxene, plagioclase, and amphibole symplectite continued during the retrograde path (1.6–0.9 GPa) at the expense of omphacite. This study shows the usefulness of evaluating the effective bulk compositions responsible for microtextural reactions; such data, combined with mineral compositions, provide quantitative thermobarometric information, even for pervasively retrogressed rocks.

Furthermore, this work reveals that the Stak massif had a metamorphic evolution similar to that of the well-preserved Kaghan and Tso Morari HP to UHP massifs in the northwest Himalaya (Guillot et al., 2008). Therefore, we propose that the Stak massif is another example of continental eclogitic metamorphism in the northwest Himalaya, and

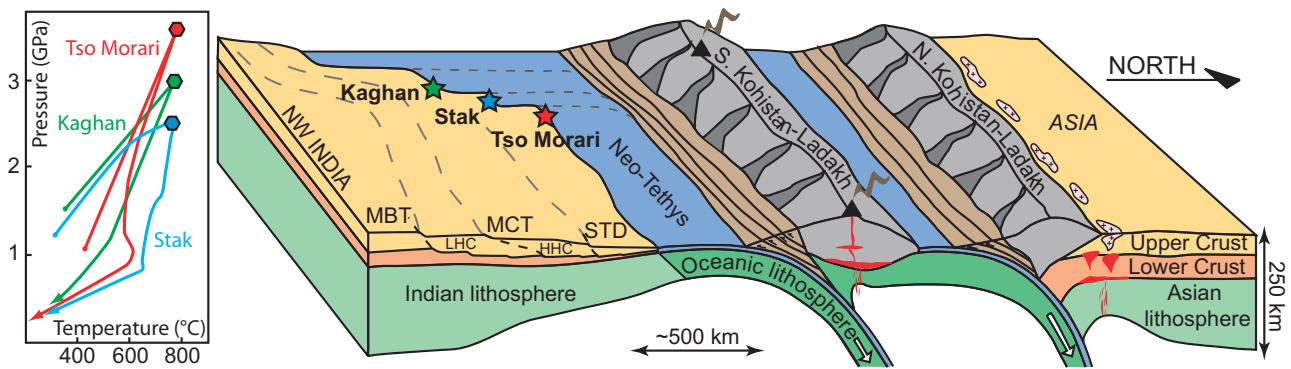


Figure 4. Schematic section of the western Himalaya during closure of the Neo-Tethys at the Paleocene-Eocene boundary, and the pressure-temperature paths for the three eclogitic units: Stak (this study), Kaghan, and Tso Morari (modified after Guillot et al., 2008). MBT—Main Boundary Thrust; LHC—Lower Himalayan crystallines; MCT—Main Central Thrust; HHC—Higher Himalayan crystallines; STD—South Tibetan detachment.

suggest that the entire northwest margin of the Indian continent records continental subduction (Fig. 4).

Worldwide, the size of UHP domains varies widely (e.g., review by Guillot et al., 2009). The Dora Maira UHP unit in the western Alps covers a surface area less than 25 km². In contrast, the Mesozoic metamorphic domain in China forms an essentially continuous HP-UHP terrane extending more than 4000 km, from Quinlin-Dabie to the Sulu belt (Yang et al., 2003). Similarly, the Western Gneiss Region in Norway forms a continuous HP-UHP unit covering more than 400 km × 200 km (Young et al., 2007). In the Himalaya, three recognized HP-UHP units (Kaghan, Stak, and Tso Morari; Fig. 1) likely form a HP-UHP terrane that is partly covered by the Kohistan-Ladakh arc and metamorphic Tethyan series. It is ~500 km long and 150 km wide (Fig. 4), which is comparable in size to the Western Gneiss Region in Norway and the Dabie-Sulu belt in China.

ACKNOWLEDGMENTS

We acknowledge A. Pourteau (University of Potsdam) for his assistance during our electron microanalysis. This work was supported by French National Research Agency (ANR) projects Cattel PAKSIS and ERD-Alps. The paper was greatly improved by constructive comments from N. Arndt, M. Leech, and two anonymous reviewers.

REFERENCES CITED

- Berman, R., 1988, Internally-consistent thermodynamic data for minerals in the system Na₂O-K₂O-CaO-MgO-FeO-Fe₂O₃-Al₂O₃-SiO₂-TiO₂-H₂O-CO₂: *Journal of Petrology*, v. 29, p. 445–522.
- Dale, J., Holland, T., and Powell, R., 2000, Hornblende-garnet-plagioclase thermobarometry: A natural assemblage calibration of the thermodynamics of hornblende: *Contributions to Mineralogy and Petrology*, v. 140, p. 353–362, doi:10.1007/s00410000187.
- De Andrade, V., Vidal, O., Lewin, E., O'Brien, P., and Agard, P., 2006, Quantification of electron microprobe compositional maps of rock thin sections: An optimized method and examples: *Journal of Metamorphic Geology*, v. 24, p. 655–668, doi:10.1111/j.1525-1314.2006.00660.x.
- de Capitani, C., and Petrakakis, K., 2010, The computation of equilibrium assemblage diagrams with Theriak/Domino software: *American Mineralogist*, v. 95, p. 1006–1016, doi:10.2138/am.2010.3354.
- Guillot, S., Mahéo, G., de Sigoyer, J., Hattori, K., and Pêcher, A., 2008, Tethyan and Indian subduction viewed from the Himalayan high- to ultrahigh-pressure metamorphic rocks: *Tectonophysics*, v. 451, p. 225–241, doi:10.1016/j.tecto.2007.11.059.
- Guillot, S., Hattori, K., Agard, P., Schwartz, S., and Vidal, O., 2009, Exhumation processes in oceanic and continental subduction contexts: A review, in Lallemand, S., and Funicello, F., eds., *Subduction zone geodynamics*: Berlin, Springer-Verlag, p. 175–204.
- Holland, T., and Blundy, J., 1994, Non-ideal interactions in calcic amphiboles and their bearing on amphibole-plagioclase thermometry: *Contributions to Mineralogy and Petrology*, v. 116, p. 433–447, doi:10.1007/BF00310910.
- Holland, T.J.B., 1990, Activities of components in omphacitic solid solutions: *Contributions to Mineralogy and Petrology*, v. 105, p. 446–453, doi:10.1007/BF00286831.
- Kotkova, J., O'Brien, P.J., and Ziemann, M.A., 2011, Diamond and coesite discovered in Saxony-type granulite: Solution to the Variscan garnet peridotite enigma: *Geology*, v. 39, p. 667–670, doi:10.1130/G31971.1.

- Lanari, P., Guillot, S., Schwartz, S., Vidal, O., Tricart, P., Riel, N., and Beysac, O., 2012a, Diachronous evolution of the alpine continental subduction wedge: Evidence from *P-T* estimates in the Briançonnais Zone houillère (France–Western Alps): *Journal of Geodynamics*, v. 56–57, p. 39–54, doi:10.1016/j.jog.2011.09.006.
- Lanari, P., Vidal, O., Schwartz, S., Riel, N., Guillot, S., and Lewin, E., 2012b, Deciphering *P-T* paths in metamorphic rocks involving zoned minerals using quantified maps (XMapTools software) and thermodynamics methods: Examples from the Alps and the Himalaya: *Geophysical Research Abstracts*, v. 14, p. 10,605.
- Le Fort, P., Guillot, S., and Pêcher, A., 1997, HP metamorphic belt along the Indus suture zone of NW Himalaya: New discoveries and significance: *Comptes Rendus de l'Académie des Sciences, Series IIA, Earth and Planetary Science*, v. 325, p. 773–778.
- Pêcher, A., Seeber, L., Guillot, S., Jouanne, F., Kausar, A., Latif, M., Majid, A., Mahéo, G., Mugnier, J.L., Rolland, Y., van der Beek, P., and Van Melle, J., 2008, Stress field evolution in the northwest Himalayan syntaxis, northern Pakistan: *Tectonics*, v. 27, TC6005, doi:10.1029/2007TC002252.
- Ravna, E.K., 2000a, Distribution of Fe²⁺ and Mg between coexisting garnet and hornblende in synthetic and natural systems: An empirical calibration of the garnet-hornblende Fe-Mg geothermometer: *Lithos*, v. 53, p. 265–277, doi:10.1016/S0024-4937(00)00029-3.
- Ravna, E.K., 2000b, The garnet-clinopyroxene Fe²⁺-Mg geothermometer: An updated calibration: *Journal of Metamorphic Geology*, v. 18, p. 211–219, doi:10.1046/j.1525-1314.2000.00247.x.
- Riel, N., Hattori, K., Guillot, S., Rayner, N., Davis, N., Latif, M., and Kausar, M., 2008, SHRIMP zircon ages of eclogites in the Stak massif, northern Pakistan: *Himalayan Journal of Sciences*, v. 5, p. 119–120.
- Schmidt, M.W., 1992, Amphibole composition in tonalite as a function of pressure: An experimental calibration of the Al-in-hornblende barometer: *Contributions to Mineralogy and Petrology*, v. 110, p. 304–310, doi:10.1007/BF00310745.
- Waters, D., 1996, The garnet-Cpx-phengite barometer: Recommended calibration and calculation method, updated 1 March 1996: <http://www.earth.ox.ac.uk/~davewa/research/eclogites/ecbarcal.html> (July 2012).
- Waters, D., 2002, Clinopyroxene-amphibole-plagioclase symplectites in Norwegian eclogites: Microstructures, chemistry and the exhumation *P-T* path: *Mineralogical Society, Winter Conference, "Timing, Transition, and Tectonics"*, Derby University, UK (abstract).
- Waters, D., 2003, *P-T* path from Cpx-Hbl-Pl symplectites, updated 22 February 2003: <http://www.earth.ox.ac.uk/~davewa/research/eclogites/symplectites.html> (July 2012).
- Waters, D., and Martin, H., 1993, Geobarometry in phengite-bearing eclogites: *Terra Nova*, v. 5, p. 410–411.
- Yang, J., Xu, Z., Dobrzinetskaya, L.F., Green, H.W., Pei, X., Shi, R., Wu, C., Wooden, J.L., Zhang, J., Wan, Y., and Li, H., 2003, Discovery of metamorphic diamonds in central China: An indication of a >4000-km-long zone of deep subduction resulting from multiple continental collisions: *Terra Nova*, v. 15, p. 370–379, doi:10.1046/j.1365-3121.2003.00511.x.
- Young, D.J., Hacker, B.R., Andersen, T.B., and Corfu, F., 2007, Prograde amphibole facies to ultrahigh-pressure transition along Nordfjord, western Norway: Implications for exhumation tectonics: *Tectonics*, v. 26, TC1007, doi:10.1029/2004TC001781.

Manuscript received 13 April 2012
 Revised manuscript received 4 July 2012
 Manuscript accepted 22 July 2012

Printed in USA